

Long-timescale simulations of H₂O admolecule diffusion on Ice Ih(0001) surfaces

Andreas Pedersen,^{1,2} Leendertjan Karssemeijer,³

Herma M. Cuppen,³ and Hannes Jónsson^{1,4}

¹*Faculty of Physical Sciences and Science Institute,
University of Iceland, 107 Reykjavík, Iceland*

²*Integrated Systems Laboratory, ETH Zurich, 8092 Zurich, Switzerland*

³*Radboud University Nijmegen, Institute for Molecules and Materials,
Heyendaalseweg 135, 6525 AJ Nijmegen, The Netherlands*

⁴*Department of Applied Physics, Aalto University, Espoo, FI-00076, Finland**

Abstract

Long-timescale simulations of the diffusion of a H₂O admolecule on the (0001) basal plane of ice Ih were carried out over a temperature range of 100 to 200 K using the adaptive kinetic Monte Carlo method and TIP4P/2005f interaction potential function. The arrangement of dangling H atoms was varied from the proton-disordered surface to the perfectly ordered Fletcher surface. A large variety of sites was found leading to a broad distribution in adsorption energy at both types of surfaces. Up to 4% of the sites have an adsorption energy exceeding the cohesive energy of ice Ih. The mean squared displacement of a simulated trajectory at 175 K for the proton-disordered surface gave a diffusion constant of $6 \cdot 10^{-10}$ cm²/s, consistent with an upper bound previously reported from experimental measurements. During the simulation, dangling H atoms were found to rearrange in order to reduce clustering, thereby approaching a linear Fletcher type arrangement. From simulations over the range in temperature, an effective activation energy of diffusion was estimated to be 0.22 eV. Diffusion on the perfectly ordered Fletcher surface was estimated to be significantly faster in the direction of the rows, with an activation energy of 0.16 eV, while diffusion perpendicular to the rows was found to be similar to that on the proton-disordered surface. Even a slight disruption of the rows of the Fletcher surface reduced the diffusivity to that on the proton-disordered surface.

INTRODUCTION

In the most common form of ice on Earth, the hexagonal Ih structure, the oxygen atoms of the water molecules reside in a hexagonal lattice. Each O atom forms four bonds in a tetrahedral arrangement with neighboring H atoms, two covalent bonds and two hydrogen bonds. One and only one H atom sits in between each pair of neighboring O atoms. As long as these *ice-rules* [1] are obeyed, the arrangement of the H atoms is rather arbitrary while the O atoms sit on a regular lattice.

Thermal energy He-atom scattering experiments [2] as well as low-energy electron diffraction (LEED) [3] indicate a full-bilayer termination of the (0001) surface at low temperature where the surface is not premelted, although the outermost molecules were not detectable by LEED because of large vibrational amplitudes [3]. When the proton-disordered ice Ih crystal is cut in between bilayers to create two surfaces, some of the hydrogen atoms of surface water molecules will not form hydrogen bonds. These dangling H atoms (DH) will form a disordered pattern on the surface. There is, however, a repulsive dipole-dipole interaction between the DHs and a lower energy ordering involves formation of rows where each DH has only two neighboring DH. This reduces the repulsion between the dipoles. Regular rows of DH on the surface of the otherwise proton-disordered ice was predicted by Fletcher to have lower energy [4]. Examples of the two types of surface structures are shown in Fig. 1. The configurational entropy of the Fletcher surface is, however, low and at finite temperature one can expect some disordering of the rows to take place. Buch *et al.* proposed that the DH form a mosaic with an intermediate degree of linear order [5] to reach a compromise between increased entropy and reduced surface energy. The He-atom scattering measurements [2] indeed revealed small features in the reflected intensity which have been interpreted in terms of regularly spaced Fletcher type rows [5]. Recently, DFT calculations have lent support for the stability of the DH ordering proposed by Fletcher [6].

The adsorption and diffusion of water admolecules on the ice surface is of central importance in the modeling of ice crystal growth, which in turn is important for predicting the shape and properties of ice particles. The diffusivity of water admolecules on the ice Ih(0001) surface at low temperature was studied experimentally by Brown and George [7] who placed an upper bound of $5 \cdot 10^{-9}$ cm²/s on the diffusion constant at 140 K. Batista and Jónsson (BJ) carried out simulations of admolecule binding and diffusion on a proton-disordered

surface using the TIP4P interaction potential and the nudged elastic band method for finding diffusion paths [8, 9] between sites identified by local energy minimization from random starting configurations. They pointed out that the DH disorder at the surface leads to a wide variety of adsorption sites, giving rise to a broad distribution of both the admolecule binding energy and the activation energy for diffusion hops between sites. The sites can be broadly classified in categories depending on how many DH are on the three underlying H₂O surface molecules. The strongest binding is obtained for sites with one or two DH, while sites with no DH bind only weakly and sites with three DHs do not provide stable binding. The disordered arrangement of the two types of sites that bind most strongly leads to irregular diffusion paths on the surface. An approximate kinetic Monte Carlo (KMC) simulation was carried out by BJ where the binding energy of a site was assigned the average value for that type of sites and the activation energy was drawn from a calculated distribution of energy barriers while the prefactor was assumed to be 10^{12} s^{-1} . From the temperature dependence of the simulated diffusivity, an effective activation energy for diffusion was estimated to be 0.18 eV and the diffusion constant $1 \cdot 10^{-9} \text{ cm}^2/\text{s}$ at 140 K, on the order of the upper bound placed by Brown and George from experimental measurements.

Nie, Bartelt and Thürmeron measured the ripening of islands on 4-5 nm thick ice films on a Pt(111) surface and interpreted the results in terms of water admolecule diffusion from small to large islands. From measurements carried out in a temperature range from 115 to 135 K, a combined activation energy for formation and diffusion of admolecules was determined to be 0.3 to 0.5 eV [10]. If the calculated estimate of the average diffusion activation energy of BJ is used, the formation energy can be estimated to be on the order of 0.1 to 0.3 eV [10]. Due to the complexity of the system, it is not clear how to interpret this quantity.

In the present paper, the results of more accurate simulations than the ones carried out by BJ are presented. They are based on the adaptive kinetic Monte Carlo method [11] (AKMC) where the mechanism and rate of diffusion events, as well as annealing events, is found from randomly initiated saddle point searches. The binding energy of the various sites found from the diffusion simulation as well as activation energy and pre-exponential factor obtained for each diffusion event are included without the averaging used by BJ. The AKMC method has previously been used, for example, in simulation studies of H atom diffusion in metal grain boundaries [12]. A more sophisticated description of the molecular interactions

was also applied, the flexible TIP4P/2005f potential function [13] instead of the original TIP4P where the geometry of the water molecules is frozen. Furthermore, the diffusion was simulated for five different models of the ordering of the DHs on the surface.

The AKMC method is a powerful method for simulating long-timescale dynamics of complex systems such as ice Ih where the proton disorder makes the simulation particularly challenging. A study of Ih(0001) surface annealing based on AKMC simulations was recently presented [14]. The applicability of the AKMC method for studies of molecular diffusion on ice surfaces was also illustrated recently by simulations of CO diffusion on the proton-disordered ice Ih(0001) surface [15].

In the following section, Section II, the simulation methodology and surface models are presented. The simulation results are presented in section III. The article concludes with a discussion and summary in Section IV.

II. METHODOLOGY

Surface models

Five models of the Ih(0001) surface with different surface DH patterns were constructed. All samples contain 360 water molecules, arranged in 6 bilayers. The z -axis is chosen to lie along the c -direction and periodic boundary conditions are applied in the plane of the surface, in the x - and y -directions, to mimic an infinite slab. The construction of each sample started from a three-dimensional ice crystal with proton disorder generated using the method of Buch *et al.* [16]. The atomic coordinates, as well as a and c lattice constants, were optimized to minimize the energy. To create the surface, two bilayers were frozen in the bulk configuration, a vacuum layer inserted below, and the four movable bilayers relaxed. The relaxed surface generated this way will be referred to as the disordered surface. To create a Fletcher surface, the same method was applied for generating a proton-disordered structure except that the hydrogen bonds between two of the bilayers were made to form rows. These two bilayers were then separated and a vacuum layer inserted. Similarly, three samples of slightly disordered Fletcher surfaces with broken rows were created, as illustrated in Fig. 1.

The inter- and intramolecular interactions were modeled with the TIP4P/2005f poten-

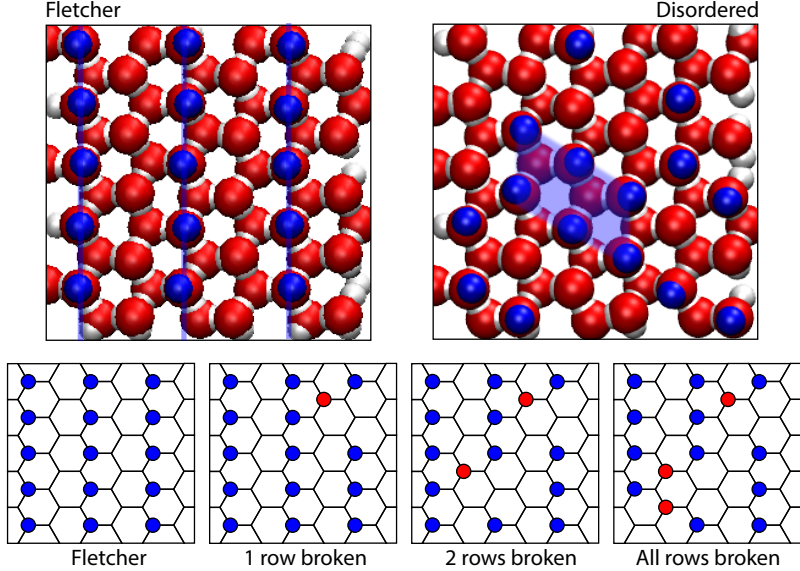


FIG. 1. Patterns of dangling H atoms (colored blue) on ice Ih(0001) surfaces used in the simulations. Upper panel: Fletcher surface and surface with disordered arrangement of dangling H atoms showing clustering in the central region. Red spheres indicate O atoms, white spheres H atoms that participate in hydrogen bonding. Lower panel: Varying degree of disorder added to the Fletcher surface. Blue circles mark dangling H atoms arranged as in the Fletcher surface, red circles denote dangling H atoms disrupting the linear ordering. The degree of deviation from the Fletcher surface is characterized in terms of the number of broken rows.

tial [13], which is a flexible version of the TIP4P/2005 potential [17]. Periodic boundary conditions were applied but the molecular interactions were smoothly brought to zero when the centers of mass of the molecules were separated by 9 to 10 Å. The relaxed, proton-disordered crystal has an a to c ratio of 1.738, which is 6.4% larger than the ratio for a perfect HCP lattice and 6.8% larger than the experimentally observed ratio for ice Ih [18].

The energy of the slab with the proton-disordered surfaces is highest, 46 meV larger than the DH ordered Fletcher surface. The slab where one DH row on the surface is broken, shown in Fig. 1, turns out to have the lowest energy, slightly lower than the perfect Fletcher surface. This illustrates the influence of the long range electrostatic field from the proton-disordered crystal slab which makes the sites on the Fletcher surface inequivalent even though the surface DH rows are ordered.

Diffusion simulation

The AKMC method [11] was used to simulate the diffusion of a single H₂O admolecule on the ice surfaces described above. The simulation starts from an energy minimized configuration where the admolecule is initially placed at a random point above the surface. A path is generated consisting of a sequence of local minima on the energy surface corresponding to adsorption sites on the substrate and first order saddle points representing transition states for diffusion hops between sites. This path represents a possible time evolution of the system over a time interval that is much longer than what could be simulated with direct classical dynamics including vibrational motion of the atoms. The EON software [19, 20] was used to conduct the simulations. For each local minimum, several searches for low lying first order saddle points were carried out using the minimum-mode following (MMF) method [21–23]. There, the eigenmode of the Hessian matrix corresponding to the lowest eigenvalue – the minimum mode – is used to transform the force acting on the atoms in such a way that the vicinity of a first order saddle point becomes analogous to that of an energy minimum. By inverting the force component parallel to the minimum mode, a climb up the potential energy surface and convergence onto a first order saddle point can be conducted by applying an ordinary minimization algorithm where the gradient of the objective function is zeroed. The minimum vibrational mode was estimated here using the Lanczos method [22, 24, 25]. After locating a saddle point, the two adjacent minima were found by displacing the system slightly along and opposite to the direction of the minimum-mode eigenvector at the saddle point followed by energy minimization. Searches for saddle points and minima were considered converged when the maximum force acting on any of the atoms dropped below 1 meV/Å. The thermal transition rate due to trajectories passing through the vicinity of each of the saddle points was estimated using harmonic transition state theory (HTST)

$$k^{\text{HTST}} = \nu \exp \left[-\frac{E_{SP} - E_R}{k_b T} \right] \quad (1)$$

$$\nu = \frac{\prod_i^D \nu_{R,i}}{\prod_i^{D-1} \nu_{SP,i}} \quad (2)$$

where E_{SP} is the energy of the saddle point, E_R is the energy of the minimum corresponding to the initial configuration, D is the number of degrees of freedom in the system, and $\nu_{SP,i}$ and $\nu_{R,i}$ are frequencies of vibrational modes at the saddle point (excluding the unstable mode, the one corresponding to the negative eigenvalue) and the reactant configuration. Several

saddle point searches were carried out for each minimum visited, until a confidence level of 0.99 was obtained as defined by Xu *et al.* [26]. Then, the simulation proceeds according to the traditional KMC algorithm by picking one of the saddle points with probability proportional to the relative rates and advancing the simulated time by

$$\Delta t = -\frac{\ln \mu}{\sum_j k_j^{\text{HTST}}}, \quad (3)$$

Here, μ is a random number in the interval $(0, 1]$ and j runs over all saddle points found on the energy ridge surrounding this minimum. After picking a transition and advancing the clock, the state of the system corresponds to the minimum on the other side of the saddle point.

The initial displacement for each saddle point search involved rotating and translating the H₂O admolecule while keeping the molecular geometry unchanged. The magnitude of the displacements was determined by values drawn from a Gaussian distributions with standard deviations of 0.25 radians and 0.25 Å. On average a total of ca. 500 saddle point searches were carried out for each minimum visited. Even though only the admolecule is displaced initially, the surface and some subsurface molecules also move during the transitions. Furthermore, annealing events that change the surface morphology are occasionally observed. A study of the annealing events was carried out separately and has been reported [14]. Here, we focus on the admolecule diffusion.

While a large speedup is gained by skipping the vibrational motion of the atoms and focusing on the rare, activated events in the AKMC simulations, the presence of fast transitions, corresponding to low activation energy, will reduce the time increment in an iteration to a small value. Even just one large value of a rate constant, k , for a possible transition in the system brings Δt , in eq 1 to a small value. In a system where there is a wide range of energy barriers as is the case for disordered systems, here the proton-disordered ice crystal, small energy barriers are likely to be present. An essential component of the simulations conducted here was a systematic coarse-graining of the energy landscape where minima separated by low energy barriers were grouped together into a single state in the list of transitions, while maintaining the correct estimate of the residence time and escape transition mechanisms from this composite state [27, 28]. The coarse-graining was limited here to include at maximum four minima to ensure sufficient resolution for determining the mean squared displacement of the admolecule. The implementation of this algorithm in

the EON software, however, allows for an arbitrary number of minima to be included in a coarse-grained state [20, 27].

The AKMC simulations typically covered time intervals on the order of $0.1 \mu\text{s}$ as determined from the sum of time increments given by eq 3. The simulated diffusion paths extended throughout the surface, *i. e.*, from one side of the simulation box to the other and, thereby, throughout the periodically replicated surface. From these paths, the possible binding sites of the admolecule were determined and rates of likely transitions involving admolecule hops between the sites as well as structural changes of the substrate. The AKMC simulation is, however, computationally demanding and the time intervals simulated here are only marginal for extracting statistically significant values of the diffusion coefficient. For the Fletcher surfaces (with and without defects) the information obtained in the AKMC simulations on binding sites and transition rates was stored and reused. The data was re-sampled in subsequent KMC simulations (without saddle point searches) covering longer time scale, from a few milliseconds at 200 K to tens of seconds at 100 K, to obtain more accurate estimates of the mean squared displacement and, thereby, more accurate values of the diffusivity. Transitions involving changes in the surface configurations were not included in the KMC simulations (unlike the AKMC simulations of the proton-disordered surface). When transition involving substrate rearrangement was drawn from the table of events, the simulation was restarted from a state where the surface had not reconstructed. This way, the diffusion constants for a given surface structure (such as a Fletcher surface with a specified number of defects) could be determined with good statistical sampling. Such simulations were carried out at 100 K, 125 K, 150 K, 175 K and 200 K including 10^8 KMC steps using the adsorption sites, and values of activation energy and pre-exponential factor obtained for each transition in AKMC simulations at 200 K.

III. RESULTS

We first discuss the adsorption energy of the H_2O admolecule at sites identified from the AKMC simulations, then the activation energy for diffusion hops, and, finally, the rate of diffusion. Results were obtained for the proton-disordered surface as well as Fletcher surfaces with various numbers of broken DH rows.

Adsorption energy

Due to the proton disorder of the ice Ih crystal, no two sites for the H₂O admolecule on the surface are the same, even for the Fletcher surface where the DHs form regular rows on the surface. The long-range electrostatic interaction from the proton-disordered crystal leads to a wide range in binding energy for the admolecule. Fig. 2 shows the distribution for the proton-disordered surface and the DH-ordered Fletcher surface. In both cases, the distribution is broad and, surprisingly, is even broader for the ordered Fletcher surface than the proton-disordered surface. On average, the binding energy of the admolecule is larger on the proton-disordered surface, consistent with the fact that it has higher surface energy.

The range in adsorption energy is so broad that a significant number of sites provide higher binding energy than the cohesive energy of the ice Ih crystal, 0.64 eV (obtained for this interaction potential function). For the proton-disordered surface, these strong binding sites are 4% of all the sites visited. This result is consistent with the findings of BJ [8, 29]. At such strong binding sites, the admolecule can form three strained hydrogen bonds with the substrate, while the cohesive energy corresponds to two hydrogen bonds [8]. Admolecules sitting in these sites will be highly stable and have little tendency to migrate to kink sites, where the binding energy will, on average, necessarily be equal to the cohesive energy. There will, of course, also be a variety of binding sites at kinks, with a broad distribution of the values of the binding energy, but the most probable state of a surface with an incomplete surface layer will have H₂O admolecules sitting at strongly binding sites on the terrace as well as at strongly binding kink sites. The time-averaged binding energy of the admolecule from the simulated path at 200 K was, indeed, found to be larger than the cohesive energy, 0.67 eV, on the proton-disordered surface showing that the admolecule spends most of its time in the strongly binding sites. On the Fletcher surface, the time-averaged binding energy at the same temperature was also large, 0.61 eV.

Diffusion hops

The proton-disordered surface of ice Ih also turns out to have a wide range in activation energy for diffusion hops of the H₂O admolecule. Fig. 3 shows the distribution of values obtained from the AKMC simulation of diffusion on the proton-disordered surface at 200 K.

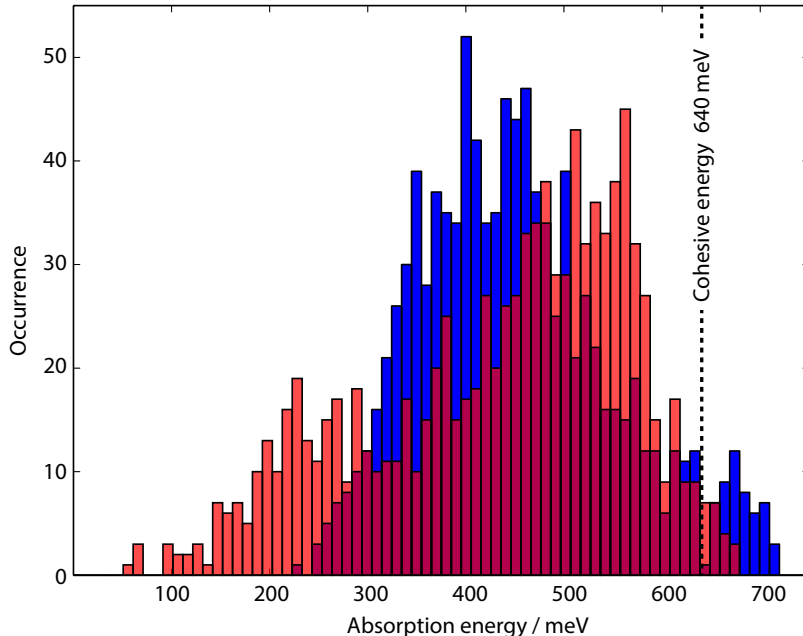


FIG. 2. Distribution of adsorption energy values obtained for a H_2O admolecule on a Fletcher surface (light red) and a surface with disordered arrangement of dangling H atoms (blue). The sites were visited during the long-timescale adaptive kinetic Monte Carlo simulation. About 4% of the sites on the disordered surface have higher binding energy than the cohesive energy of ice Ih, which was calculated to be 0.64 eV using the TIP4P/2005f interaction potential function. On average the binding energy is larger on the disordered surface, consistent with the higher surface energy.

Most of the transitions have a low activation energy, below 0.1 eV, but a significant number of transitions have an activation energy between 0.1 and 0.2 eV. Transitions with even higher activation energy were occasionally also selected to be part of the AKMC path, but only rarely. There is a finite probability that the random number drawn to select the next transition in the path points to a mechanism that involves relatively high activation energy. The coarse-graining where minima separated by a low energy barrier are grouped together in a single state also reduces the occurrence of transitions with low activation energy. When two or more minima have been grouped together in the coarse-graining, the activation energy of an escape event is recorded as the energy of the saddle point minus the energy of the lowest minimum in the group.

The mechanism of these transitions is similar to what has been presented previously by

BJ. As the admolecule moves from one site to another, the underlying surface molecules typically rotate to maintain hydrogen bonding. It is, therefore, extremely important not to artificially constrain the surface molecules and allow several layers in the ice lattice to relax during the climb up the potential surface to saddle points [8]. The diffusion hops did not, however, involve concerted displacements where the admolecule replaced a surface molecule, a mechanism that has been found to be important in metal adatom diffusion [28, 30, 31]. Such concerted displacement events have, nevertheless, been found to be the prevailing mechanism of annealing events in the surface layer of ice Ih [14].

The pre-exponential factor in the HTST expression, eq 2, for the rate constant of diffusion hops was evaluated from the vibrational frequencies obtained by constructing the Hessian matrix for all degrees of freedom in the system. Calculations based on a sub-matrix, including only the atoms displaced most, turned out not to satisfy detailed balance well enough to be applied in the KMC resampling simulations. A slight drift in the diffusion paths resulted from a violation of detailed balance. The prefactors were typically found to be on the order of 10^{13} s^{-1} .

Diffusion constants

The mean squared displacement calculated from a path generated from an AKMC simulation of diffusion on the proton-disordered surface at 175 K is shown in Fig. 4. While the statistical fluctuations are large, the long time results can be fitted to a straight line to estimate a diffusion coefficient according using the Einstein-Smoluchowski equation

$$D = \frac{\langle |\mathbf{r}(t_0 + \tau) - \mathbf{r}(t_0)|^2 \rangle}{2d\tau}, \quad (4)$$

where d is the number of dimensions, $d = 2$ in the present case. This gives a diffusion coefficient of $D = 6 \cdot 10^{-10} \text{ cm}^2/\text{s}$.

An inspection of the surface before and after the diffusion simulation reveals that significant changes have occurred in the DH pattern, as shown in Fig. 5. While the ordering of the original disordered surface involves a cluster of DHs, with one of them surrounded by five DHs at nearest neighbor sites, the final configuration has a more linear ordering where there are at most three nearest neighbor DHs. This can be seen as an evolution of the proton-disordered surface towards a Fletcher-type surface. Most of these annealing transitions occurred early on in the simulation and do not affect the long range linear fit used to

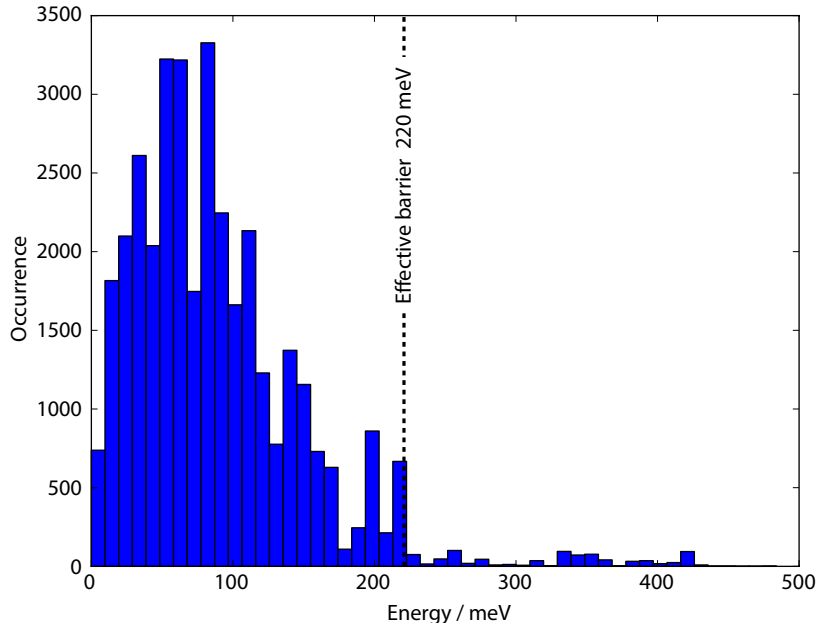


FIG. 3. Distribution of activation energy values for H_2O admolecule diffusion hops on the proton-disordered surface at 200 K. The values were obtained from long-timescale adaptive kinetic Monte Carlo simulations of the diffusion. While most of the values are below 0.1 eV, transitions with energy over 0.2 eV turn out to be essential for obtaining a diffusion path extending over the full width of the simulated surface.

determine the diffusion constant. While the initial states in the MMF saddle point searches only involve displacement of the admolecule, the surface molecules (as well as molecules in layers further down from the surface) are free to move and rotate and in some of the transitions the DH pattern on the surface changed. Such annealing transitions have been discussed previously [14]. The focus here will be on the diffusivity of the H_2O admolecule.

Similar simulations were carried out for the Fletcher surface and defected Fletcher surfaces (shown in Fig. 1). Also there, annealing events that change the DH ordering occasionally occur. In order to extract accurate diffusion constants for surfaces with a certain, well defined arrangement of DHs, the annealing events were excluded from the table of possible transitions. Also, in order to obtain better statistics for the mean squared displacement and the deduced diffusion constant, regular KMC simulations were carried out for long time intervals after mapping out the possible adsorption sites and likely diffusion hops with AKMC simulations. Two such paths simulated at 150 K are shown in Fig. 6 where the admolecule has moved over distances on the scale of micrometers. The anisotropy of the

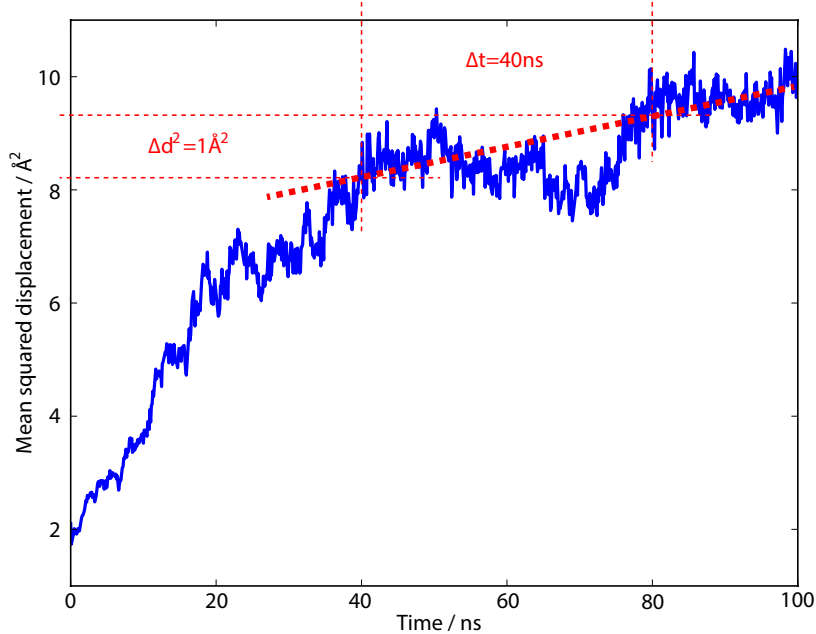


FIG. 4. Mean squared displacement of an H_2O ad molecule on the proton-disordered surface as a function of time obtained from the adaptive kinetic Monte Carlo simulation spanning 100 ns time interval at 175 K. From the long time slope of the curve, a diffusion coefficient of $D = 6 \cdot 10^{-10} \text{ cm}^2/\text{s}$ is obtained.

diffusion on the Fletcher surface is evident from the figure, the diffusion being faster and the paths extending further in the direction along DH rows. In order to characterize the anisotropy of the diffusion on the Fletcher surface, the mean squared displacement parallel and perpendicular to the DH rows were calculated separately and the long time results fitted by a straight line to extract a diffusion constant using eq 3 with $d = 1$. Fig. 7 shows an example of such a calculation, the mean squared displacement along rows obtained from three independent simulations at 100 K. For each curve a linear fit of the long time values was used to extract a diffusion constant and then an average taken of the values obtained from the three curves. By calculating separately the mean squared displacement parallel and perpendicular to the rows, a parallel diffusion constant, D_{\parallel} , and a perpendicular diffusion constant, D_{\perp} were thus obtained from such simulations.

Fig. 8 shows results obtained for the diffusion constant D_{\parallel} at various temperature values ranging from 100 to 200 K. The diffusion constant is found to vary with temperature according to the Arrhenius equation and the slope of the lines gives the activation energy of diffusion in each of the two directions. The activation energy for diffusion is 0.22 eV for

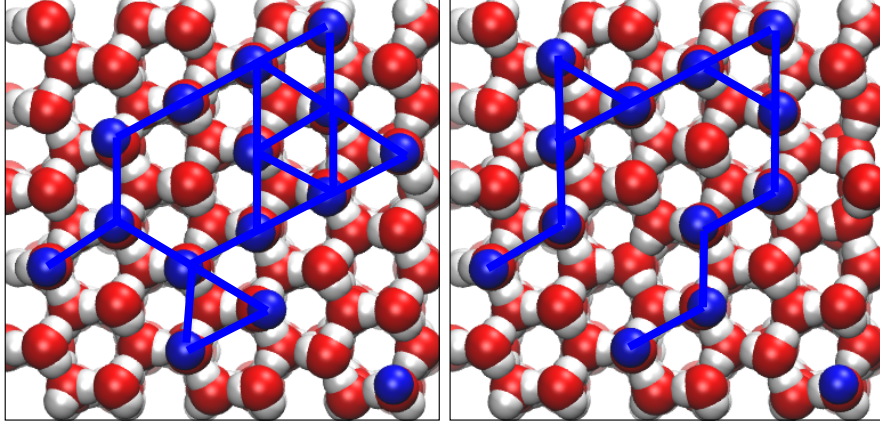


FIG. 5. Arrangement of dangling H atoms before (left) and after (right) an adaptive kinetic Monte Carlo simulation of H_2O admolecule diffusion on the proton-disordered surface. The color code is the same as in Fig. 1. A blue line is drawn between dangling H atoms located on adjacent sites. The initial clustering of the dangling H atoms is reduced during the diffusion simulation as the surface energy is lowered by spacing them further apart. Since the substrate molecules are free to move in the saddle point searches, surface rearrangement processes are included in the table of possible transitions, even though only the admolecule is initially displaced.

diffusion perpendicular to the rows, but 0.16 eV for diffusion parallel to the rows. The values are listed in Table 1, along with the ratio of the diffusion constants, $r = D_{\parallel}/D_{\perp}$, at 100 to 200 K. These results show that the diffusion on the Fletcher surface is highly anisotropic, being three orders of magnitude faster along the DH rows than perpendicular to the rows at 100 K and a factor of 24 faster at 200 K.

The perfect Fletcher surface is, however, not the most stable arrangement of the DHs. A slightly lower energy ordering was found by breaking one of the rows and placing a DH in between rows, as shown in Fig. 1. Such defective Fletcher surfaces have, furthermore, larger entropy and will, thereby, have lower free energy at finite temperature than the perfect Fletcher surface. We now address how such defects affect the diffusivity. Results of simulations of diffusion on Fletcher surfaces with one, two and three broken rows (*i. e.*, all three rows in the simulation cell) are shown in Fig. 8. Again, clear Arrhenius dependence on temperature is obtained and the extracted values of the activation energy are listed in Table 1. The low activation energy for diffusion along rows on the perfect Fletcher surface increases as more of the rows are broken and DHs placed between the rows. When all three rows have

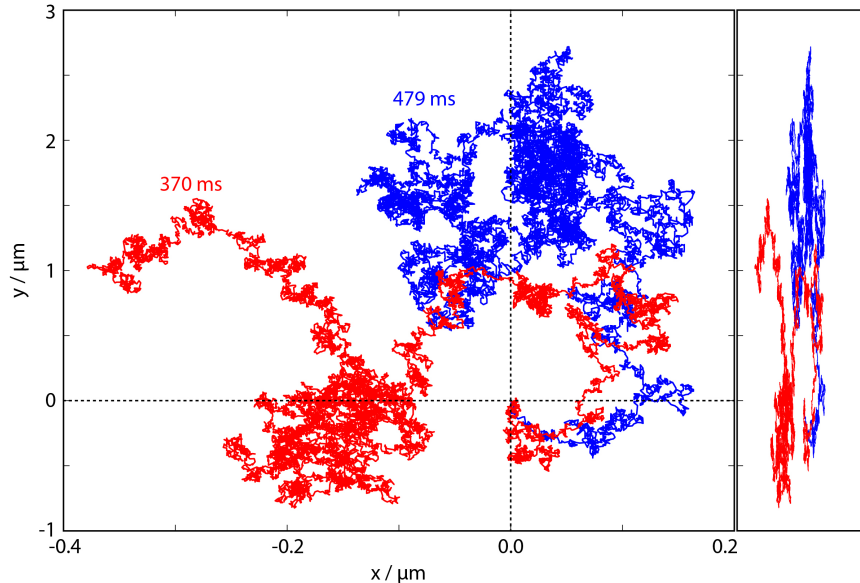


FIG. 6. Two simulated diffusion paths of an H_2O admolecule on a Fletcher surface with unbroken rows of dangling H atoms at 150 K. In the left figure, the scale of the graph corresponding to the distance perpendicular to the rows, x , is chosen to be different from the one parallel to the rows, y , to clearly display the trajectories. In the right figure, the scale is the same and the strong anisotropy of the diffusion can be seen clearly, The diffusivity along the rows is 70 times higher than diffusivity perpendicular to the rows.

been broken, the activation energy for diffusion parallel to the rows equals the activation energy for diffusion perpendicular to the rows. The anisotropy is, thereby, eliminated by just a single DH between each of the rows. The diffusion on such a slightly disordered Fletcher surface is quite similar to the diffusion on the annealed, proton-disordered surface.

IV. DISCUSSION AND SUMMARY

The study presented here of H_2O admolecule diffusion on the ice Ih(0001) surface improves upon and extends the early simulation study of BJ [8]. A more sophisticated simulation methodology is used, regarding both the simulation algorithm and the interaction potential. Also, the effect of DH ordering is studied, ranging from perfect rows of DHs on the Fletcher surface, to a Fletcher surface where all rows are broken, and a (annealed) proton-disordered surface. The results are consistent with published measurements of Brown and George in that the diffusion constant for the most likely models of the ice surface, an annealed proton-

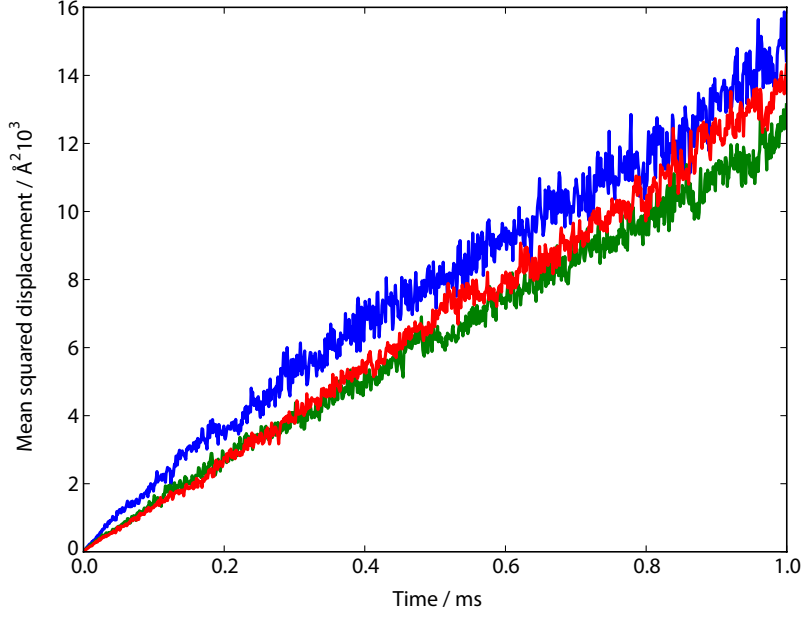


FIG. 7. Mean squared displacement along rows of dangling H atoms of the Fletcher surface obtained from simulations for 100 K. Results of three independent calculations are shown. The average diffusion constant deduced from these simulations is shown in Fig. 8 along with analogous results for higher temperature and for different surfaces.

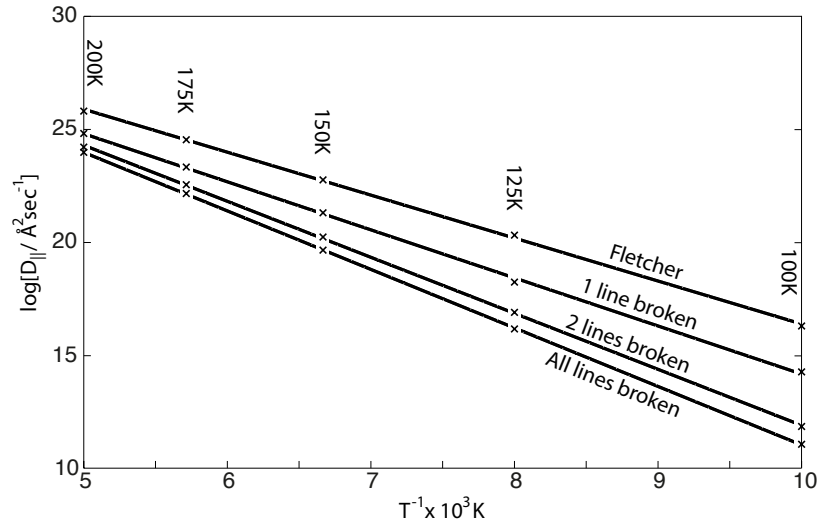


FIG. 8. Diffusion coefficient obtained from the mean squared displacement of the admolecule parallel to the rows of dangling H atoms on the Fletcher surface with regular, unbroken rows as well as defected Fletcher surfaces where one or more dangling H atom is placed in between the rows (as shown in Fig. 1) as a function of inverse temperature over the range 100 to 200 K.

TABLE I. Activation energy of surface diffusion of an H₂O molecule on ice Ih(0001) surface and ratio of diffusion rate parallel and perpendicular, $r = D_{\parallel}/D_{\perp}$ to rows of dangling H atoms on the perfect and distorted Fletcher surface models. The activation energy was obtained from the temperature dependence of the diffusivity over a temperature range from 100 to 200 K. The ratio, r , is given for the highest and lowest temperature.

	E_{\perp}^a	E_{\parallel}^a	r_{100K}	r_{200K}
Fletcher	0.22 eV	0.16 eV	570	24
1 row broken	0.23 eV	0.18 eV	180	13
2 rows broken	0.25 eV	0.21 eV	16	4
all rows broken	0.22 eV	0.22 eV	1	1

disordered surface or disordered Fletcher surface (all rows broken), are about an order of magnitude smaller than the upper bound set by the experimental results [7].

The adsorption energy is found to vary greatly from one site to another due to the proton disorder in the ice lattice, with ca. 4% of the sites on the proton-disordered surface providing larger binding energy than the cohesive energy of the crystal. Even the perfectly ordered Fletcher surface has a broad distribution in adsorption energy because of the long range electrostatic interaction as well as the variation in the number of DHs at the nearest molecules in the surface layer. Admolecules sitting in these strongly binding sites will be highly stable and not have a tendency to migrate to kink sites, where the binding energy will, on average, necessarily be equal to the cohesive energy. There will, of course, also be a distribution of binding energy of an H₂O molecule at kink sites, but the most common situation of a surface with an incomplete surface layer will have admolecules sitting at strongly binding kink sites as well as strongly binding sites on the flat terrace. As a result, the terraces will not be free of admolecules, even when the temperature is high enough for diffusion from terrace sites to step and kink sites to be possible. It has been suggested [8] that this could explain the observation of dispersionless modes in inelastic He-atom scattering [2] since the vibration of isolated admolecules is likely to couple only weakly to the vibrations of the crystal lattice.

The diffusion is found to be highly anisotropic on the perfect Fletcher surface, with the

ratio of diffusion parallel and perpendicular to the rows ranging from 24 at 200 K to 570 at 100 K. However, only a slight disordering of the Fletcher surface, obtained by placing a few DHs in between the rows, a likely configuration at finite temperature because of both energetic and entropic considerations, eliminates the anisotropy. These findings indicate that it will be difficult to observe experimentally an anisotropy in admolecule diffusion on an Ih(0001) surface even if the DHs are close to being ordered in Fletcher rows. Only a slight deviation from the perfect order leads to isotropic diffusion.

The average activation energy for diffusion on the proton-disordered surface and the Fletcher surface with all rows broken was determined to be 0.22 eV from the variation of the diffusion constant over the temperature interval from 100 to 200 K. The time averaged binding energy of the H₂O molecule on the surface calculated over a diffusion path obtained at 200 K was found to be 0.67 eV. The ratio of the diffusion activation energy to the desorption activation energy is, therefore, found to be 1/3. This is an important quantity that enters, for example, in the modeling of ice crystal growth.

The quantitative accuracy of the results obtained here could, however, be improved. The simulations presented here made use of a simple, point charge model for the H₂O intermolecular interaction. Further work, using a more accurate description, such as the single center multipole expansion (SCME) potential [32] would be desirable. The SCME potential gives better agreement with the experimental lattice constants and cohesive energy of ice Ih than the potential function used here. The multipole expansion used in the SCME potential also gives electrostatics in good agreement with *ab initio* and density functional theory calculations [33]. It would, therefore, be interesting to repeat the types of simulations carried out here with the SCME potential.

It would also be interesting to assess whether quantum mechanical effects would alter the results obtained here since the simulations were based on a classical description of the atoms. The binding energy and the transition rates can be affected by the quantum delocalization of the protons. Such a simulation could be carried out using harmonic quantum transition state theory where zero point motion and quantum tunneling is taken into account. The AKMC method can, in principle, be extended in this way and simulations can be carried out where the effect of quantum tunneling on the transition rates is included [28].

A.P. and H.J. were supported by the Icelandic Research Fund and the University of Iceland Research Fund. L.J.K and H.M.C were supported by the European Research Council

(ERC-2010-StG, Grant Agreement No. 259510-KISMOL). H.M.C. thanks The Netherlands Organization for Scientific Research (NWO) (VIDI 700.10.427), A.P. and H.J. thank Jean-Claude Berthet for helpful discussions, and A.P. thanks COST Action CM0805 for travel funds.

* hj@hi.is

- [1] J. D. Bernal and R. H. Fowler, *J. Chem. Phys.* **1**, 515 (1933).
- [2] A. Glebov, A. Graham, A. Menzel, J. Toennies and P. Senet, *J. Chem. Phys.* **112**, 11011(2000).
- [3] N. Materer, U. Starke, A. Barberi, M. A. Van Hove, G. A. Somorjai, G.-J. Kroes, and C. Minot, *Surf. Sci.* **381**, 190 (1997).
- [4] N. H. Fletcher, *Philos. Mag. B* **66**, 109 (1992).
- [5] V. Buch, H. Groenzin, I. Li, M. J. Shultz and E. Tosatti, *Proc. Natl. Acad. Sci.* **105**, 5969 (2008).
- [6] D. Pan, L-M. Liu, G. A. Tribello, B. Slater, A. Michaelides and E. G. Wang, *J. Phys.: Condens. Matter* **22**, 074209 (2010).
- [7] D. E. Brown and S. M. George, *J. Phys. Chem.* **100**, 15460 (1996).
- [8] E. R. Batista and H. Jónsson, *Comp. Mat. Sci.* **20**, 325 (2001).
- [9] E. R. Batista, Ph.D. thesis, University of Washington (1999).
- [10] S. Nie, N. Bartelt, and K. Thürmer. *Phys. Rev. Lett.* **102**, 136101 (2009).
- [11] G. Henkelman and H. Jónsson, *J. Chem. Phys.* **115**, 9657 (2001).
- [12] A. Pedersen and H. Jónsson, *Acta Materialia* **57**, 4036 (2009).
- [13] M. A. González and J. L. F. Abascal, *J. Chem. Phys.* **135**, 224516 (2011).
- [14] A. Pedersen, K. T. Wikfeldt, L.J. Karssemeijer, H. Cuppen and H. Jónsson, *J. Chem. Phys.* **141**, 234706 (2014).
- [15] L.J. Karssemeijer, A. Pedersen, H. Jónsson and H. M. Cuppen, *Phys. Chem. Chem. Phys.* **14**, 10844 (2012).
- [16] V. Buch, P. Sandler and J. Sadlej, *J. Phys. Chem. B* **102**, 8641 (1998).
- [17] J. L. F. Abascal and C. Vega. *J. Chem. Phys.* **123**, 234505 (2005).
- [18] K. Röttger, A. Endriss, J. Ihringer, S. Doyle and W. F. Kuhs, *Acta Crystallogr B.* **68**, 91 (2012).
- [19] A. Pedersen and H. Jónsson, *Math. Comput. Simul.* **80**, 1487 (2010).
- [20] S.T. Chill, M. Welborn, R. Terrell, L. Zhang, J-C. Berthet, A. Pedersen, H. Jónsson and G. Henkelman, *Modelling Simul. Mater. Sci. Eng.* **22**, 055002 (2014).

- [21] G. Henkelman and H. Jónsson, *J. Chem. Phys.* **111**, 7010 (1999).
- [22] R. Olsen, G. J. Kroes, G. Henkelman and H. Jónsson, *J. Chem. Phys.* **121**, 9776 (2004).
- [23] A. Pedersen, S. F. Hafstein, and H. Jónsson, *SIAM J. Sci. Comput.* **33**, 633 (2011).
- [24] J. Tennyson, *Computer Physics Reports* **4**, 36 (1986).
- [25] R. Malek and N. Mousseau, *Phys. Rev. E* **62**, 7723 (2000).
- [26] L. Xu and G. Henkelman. *J. Chem. Phys.* **129**, 114104, 2008.
- [27] A. Pedersen, J-C. Berthet and H. Jónsson, *Lect. Notes in Comp. Sci.* **7134**, 34 (2012).
- [28] H. Jónsson, *Proc. Natl. Acad. Sci.* **108**, 944 (2011).
- [29] E. R. Batista and H. Jónsson, *Comp. Mat. Sci.*, *Corrigendum* (in press, 2015).
- [30] P.J. Feibelman, *Phys. Rev. Lett.* **65**, 729 (1990).
- [31] M. Villarba and H. Jónsson, *Surf. Sci.* **317**, 15 (1994); *Phys. Rev. B* **49**, 2208 (1994).
- [32] K. T. Wikfeldt, E. R. Batista, F. D. Vila and H. Jónsson, *Phys. Chem. Chem. Phys.* **15**, 16542 (2013).
- [33] E. R. Batista, S. Xantheas and H. Jónsson, *J. Chem. Phys.* **111**, 6011 (1999).